Journal of South American Earth Sciences 50 (2014) 1–11

Contents lists available at ScienceDirect

Journal of South American Earth Sciences

journal homepage: www.elsevier.com/locate/jsames

New data on neotectonic contractional structures in Precordillera, south of Río de La Flecha: Structural setting from gravity and magnetic data. San Juan, Argentina

Laura P. Perucca [a,*], Francisco Ruiz [b]

[a] Gabinete de Neotectónica y Geomorfología, INGEO-FCEFyN-UNSJ, CONICET, Av. Ignacio de La Roza y Meglioli 5400 San Juan, Argentina
[b] Instituto Geofísico Sismológico Volponi, Facultad de Ciencias, Exactas, Físicas y Naturales, Universidad Nacional de San Juan, Argentina

ARTICLE INFO

Article history:
Received 23 April 2013
Accepted 19 November 2013

Keywords:
Quaternary faults
Opposite vergence
Triangle zone axis
Geophysical data
Argentinean Precordillera

ABSTRACT

The Central and Eastern Precordillera form oppositely verging thrust systems on the western and eastern sides of the Matagusanos-Maradona-Acequión valley, establishing a thick-skinned triangle zone with significant changes in the axis position along strike. Between the del Agua and the de La Fecha rivers, the axis of this triangular zone is located in the eastern portion of the depression. Changes in the position of the triangle zone axis along strike, whether to the east or to the west, took place during Pliocene–Pleistocene times. Geophysical and geodetic data indicate a subsurface structure striking NE, oblique to the general direction of the foreland with dextral displacement. Accordingly, the change in the location of the triangular area could be attributed to stress transfer controlled by heterogeneities in the basement. By analytic signal analysis of magnetic anomalies, it is possible to assess the regional structural coupling between Pie de Palo and Eastern Precordillera. The oblique arrangement of basement blocks could explain transverse lineaments and the sigmoidal geometry of the Eastern Precordillera. Geophysical and geological evidence shows that the depression is crossed by several E–W strike-slip faults. These faults possibly controlled the position of the triangle zone axis until Neogene–Pleistocene times by transferring displacements and provoking its jump along strike.

Basement structures might have also played a primary role in the location of Quaternary faults trending N–S. Finally, the east–west cross-section geophysical model shows the triangular zone, responding to the different controls imposed by the pre-existing basement structures.

1. Introduction

Between 27° and 33° South latitude and with a convergence azimuth of around 78° (Vigny et al., 2009) (Fig. 1a and b), the Nazca plate is being subducted at a rate of 6.3 cm/year beneath the South American plate to depths of up to 100 km (Barazangi and Isacks, 1976; Pilger, 1981; Ramos, 1988; Kendrick et al., 2003). The flat geometry of the subducted slab is attributed to the oblique subduction of the Juan Fernández ridge beneath the South American plate (Pilger, 1981; Yañez et al., 2001; Anderson et al., 2007; Alvarado et al., 2009; Martinod et al., 2010; Rosenbaum and Mo, 2011). In this area, Late Miocene–Quaternary tectonics have resulted in the development of the Principal and Frontal Cordilleras, Precordillera and the Sierras Pampeanas in the eastward foreland region (Ramos, 1988) (Fig. 1b). Beck et al. (2008) and Alvarado et al. (2009) refined the location of earthquakes in the flat-slab near 30°–31°S and showed that the shallowest portion of the slab is associated with the subducting Juan Fernandez ridge.

The convergence between the Nazca and South America plates resulted in a thin-skinned fold-and-thrust belt in the Central Precordillera, and a thick-skinned tectonic style in the Sierras Pampeanas (Jordan et al., 1983b; Jordan and Allmendinger, 1986; Smalley et al., 1993; Ramos et al., 2002; among others). Therefore, the Eastern Precordillera and the western Pampean Ranges are made of a west-verging thrust system, whilst the Central Precordillera comprises east-vergence thrusts (Figueroa and Ferraris, 1989; Von Gosen, 1992; Ramos et al., 1997). These two morphostructural units, with opposite vergences, formed a thick-skinned triangle zone, with its Eastern side involving foreland basement in the deformation (Jordan et al., 1993; Zapata and Allmendinger, 1996a, b). According to Zapata and Allmendinger (1996b), this thick-skinned triangle zone began to grow at 2.6 Ma and seismic activity also shows that deformation of the Eastern Precordillera is still active (Smalley et al., 1993). However, Meigs et al. (2006) and

* Corresponding author.
E-mail addresses: lperucca@unsj-cuim.edu.ar, lauraperucca@yahoo.com.ar (L. P. Perucca), fruiz@unsj-cuim.edu.ar (F. Ruiz).

0895-9811/$ – see front matter © 2013 Elsevier Ltd. All rights reserved.
http://dx.doi.org/10.1016/j.jsames.2013.11.006

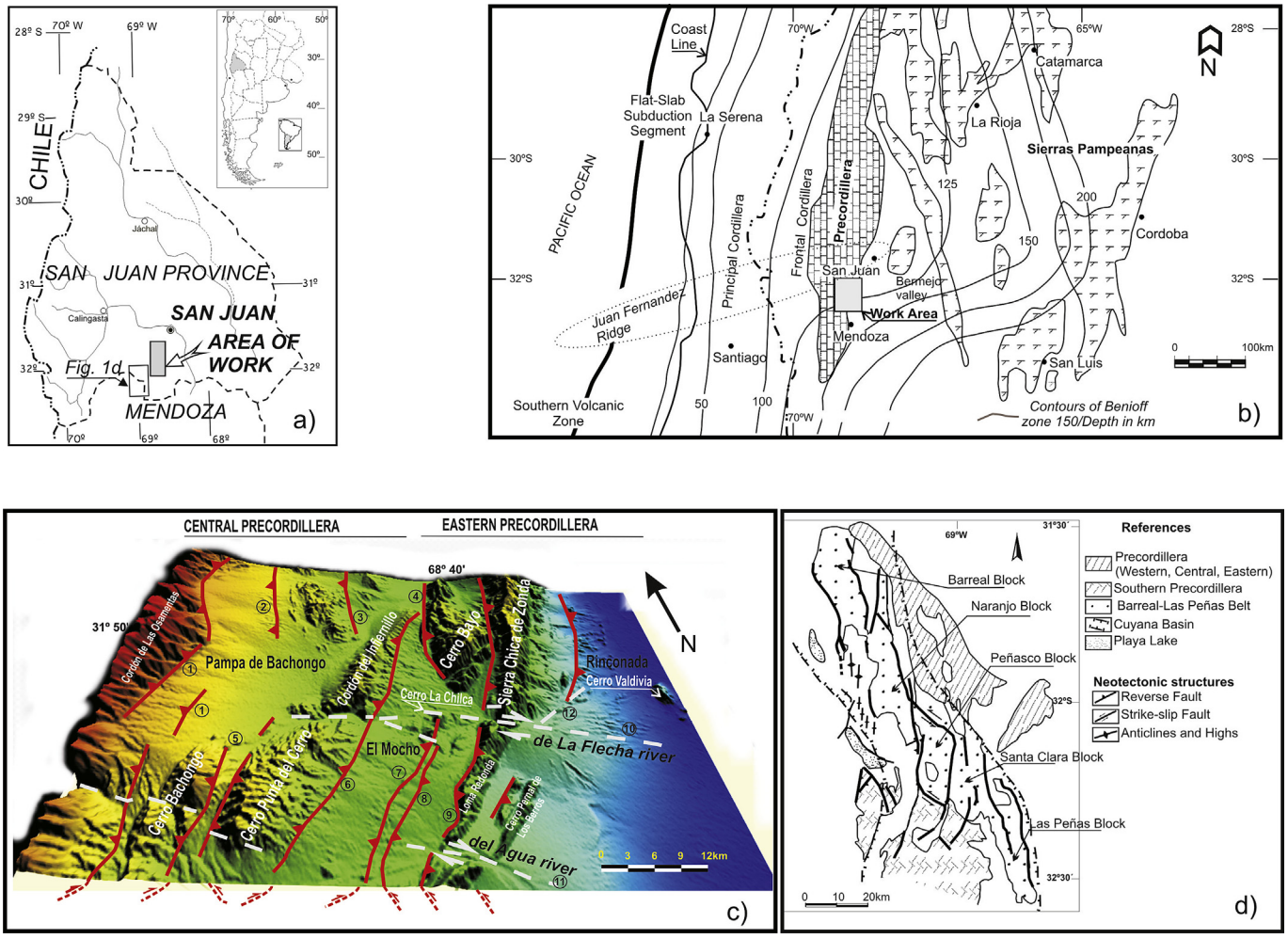

Fig. 1. (a) Map showing the relative location of San Juan province in Argentina and South America, and (d) (Barreal-Las Peñas Belt situation). (b) Location of the Pampean flat-slab segment between 28° and 32° S with depth-contours of the oceanic slab (modified from Ramos et al., 2002), (c) location Map and shaded-relief image of 90 m-spacing digital elevation model (DEM derived from SRTM data), highlighting the structural and neotectonic array of the interaction between main thrusts. 1 – Las Osamentas thrust, 2 – Maradona fault, 3 – Papagallos fault, 4 – Cerro Bayo thrust, 5 – Cerro Bachongo thrust, 6 – Cerro Punta del Cerro thrust, 7 – Cerro La Chilca Fault, 8 – El Mocho fault, 9 – Zonda-Pedernal thrust, 10 – La Flecha fault, 11 – Guanacache fault, and 12 – Cruz de Caña fault. (d) Geological scheme of Barreal-Las Peñas Belt situation (modified from Cortés et al., 2006).

Vergés et al. (2007) interpreted that the Eastern Precordillera faults are back thrusts triggered by basement wedging caused by a low-angle, east-verging blind fore-thrust ramp at depth and the western vergence of Eastern Precordillera is apparent.

This study aims at interpreting the geometry of neotectonic deformations developed in the linkage zone between antithetic thrust systems of different nature and its evolution among oblique E–W faults, as described above. A further aim is to contribute to a better understanding of the Quaternary tectonic evolution of this segment of the Andean thrust front.

In this paper, gravity and magnetic analyses have been used to define the subsurface structure of the area and to obtain information on location, density and magnetization distribution of the upper crust in the Precordillera and western Sierras Pampeanas of San Juan. The magnetic analytic signal (Nabighian et al., 2005) superimposed on a geological structural map allows a strengthened interpretation of lineaments associated with Quaternary tectonic activity.

2. Geological and neotectonic setting

The study area is located in the south-central region of the province of San Juan, Argentina, about 50 km SW of the city of San Juan (Fig. 1a). It comprises the transition zone between the Precordillera and western Sierras Pampeanas within the active deformation belt of the southern central Andes (Fig. 1b).

The Central Precordillera is formed by mountain ranges running from latitudes 29° to 32°S. It has been described by several authors (Jordan et al., 1983a; Allmendinger et al., 1990; Von Gosen, 1992; Jordan et al., 1993; Cristallini and Ramos, 2000) as a typical thin-skinned thrust-and-fold belt due to Neogene crustal shortening on west dipping, imbricated structures that root down to a 10–15 km deep main decollement (Fig. 1c).

The ranges forming the Eastern Precordillera trend N–S and these outcropping structures are in general large asymmetric anticlines, whose axes are sub-parallel to the mountain chains. Their axial planes are steeply inclined to the east, and most of their western flanks are vertical, overturned or have been eliminated by high angle reverse faults sub-parallel to the structural axes. The longest of these faults corresponds to the western limit of the Eastern Precordillera (Villicum-Zonda-Pedernal thrust), highlighting the sinusoidal shape of Eastern Precordillera at Sierra Chica de Zonda (Figs. 1c and 2a).

The Sierras Pampeanas basement appears to influence the geometry of the structures reactivated during the Pliocene–

Pleistocene at the Eastern Precordillera, since the development of flat subduction, therefore inducing modifications in the style of compressive deformation within the Precordillera fold-and-thrust belt (Jordan et al., 1983a; Ramos et al., 2002; Zambrano and Suvires, 2008).

Siame et al. (2006) described the role of Pie de Palo in the partitioning of the Plio-Quaternary deformations, within the structural context of the Andean back-arc at about 31°S. La Flecha fault, trending N70°W, nearly perpendicular to the N–S structures has been recognized in the area, with a dextral slip (Vaca, 1977). Zambrano and Suvires (2008) analyzed information from electrical resistivity geophysical measurements and wells drilled for ground water in the Tulum Valley pointing out the Quaternary activity of the La Flecha fault.

Several evidence of Quaternary activity for this structure has been recognized in the La Flecha river area. For example, W–E calcite-filled veins with horizontal fresh striae were recognized in the northern portion of cerro La Flecha (Figs. 3a and 4a); besides, W–E trending brecciated trachyte dikes of Triassic age (Castro de Machuca et al., 2013) were located in the contact between the trachytes dikes and Ordovician limestones, indicating a post-Triassic tectonic activity (Figs. 3a and 4b). Further west, several faults with trends from 100° to 130° and dips from 45° to 89° south and north affect Neogene rocks (Figs. 3a and 4c). Further west, an E–W trending Quaternary fault places a vein of calcite over Quaternary alluvial deposits (Figs. 3a and 4d), at the northwestern flank of cerro La Chilca. Here, the 65°N dipping plane trending 100° intersects a vein of calcite (Paleozoic) over Quaternary deposits.

Other evidence of transversal Quaternary faulting was identified to the north of the La Flecha River, on the eastern piedmont of Sierra Chica de Zonda. In this area, Vaca (1977) and Martos (1995) described the Cruz de Caña fault, that trends N50°E with an uphill-facing fault scarp (Figs. 1c and 2a). Martos (1995) recognized at least four fault reactivations from the Middle Pleistocene to the Holocene. The Cruz de Caña reverse fault dips 60° SE and according to Martos (1995) shows evidence of dextral displacement.

Further south and coincident with the Del Agua River, Zambrano and Suvires (2008) described another E–W structure, called the Guanacache mega-fracture, to which they assign a dextral displacement (Fig. 2a and b). They established that the N–S Tulum fault system results in a tectonic horst structure, segmented by many normal and/or strike slip faults transverse or oblique to the horst strike (Fig. 2b). They interpreted a change to compressive tectonics beginning with the Miocene and inferred that these faults had tectonic activity during the Quaternary.

Cortés et al. (2006) recognized in the eastern flank of the Central Andes, between 31° 30′ and 33° 30’ SL, a regional NW striking structure, called the Barreal-Las Peñas belt (Figs. 1d and 2b). The

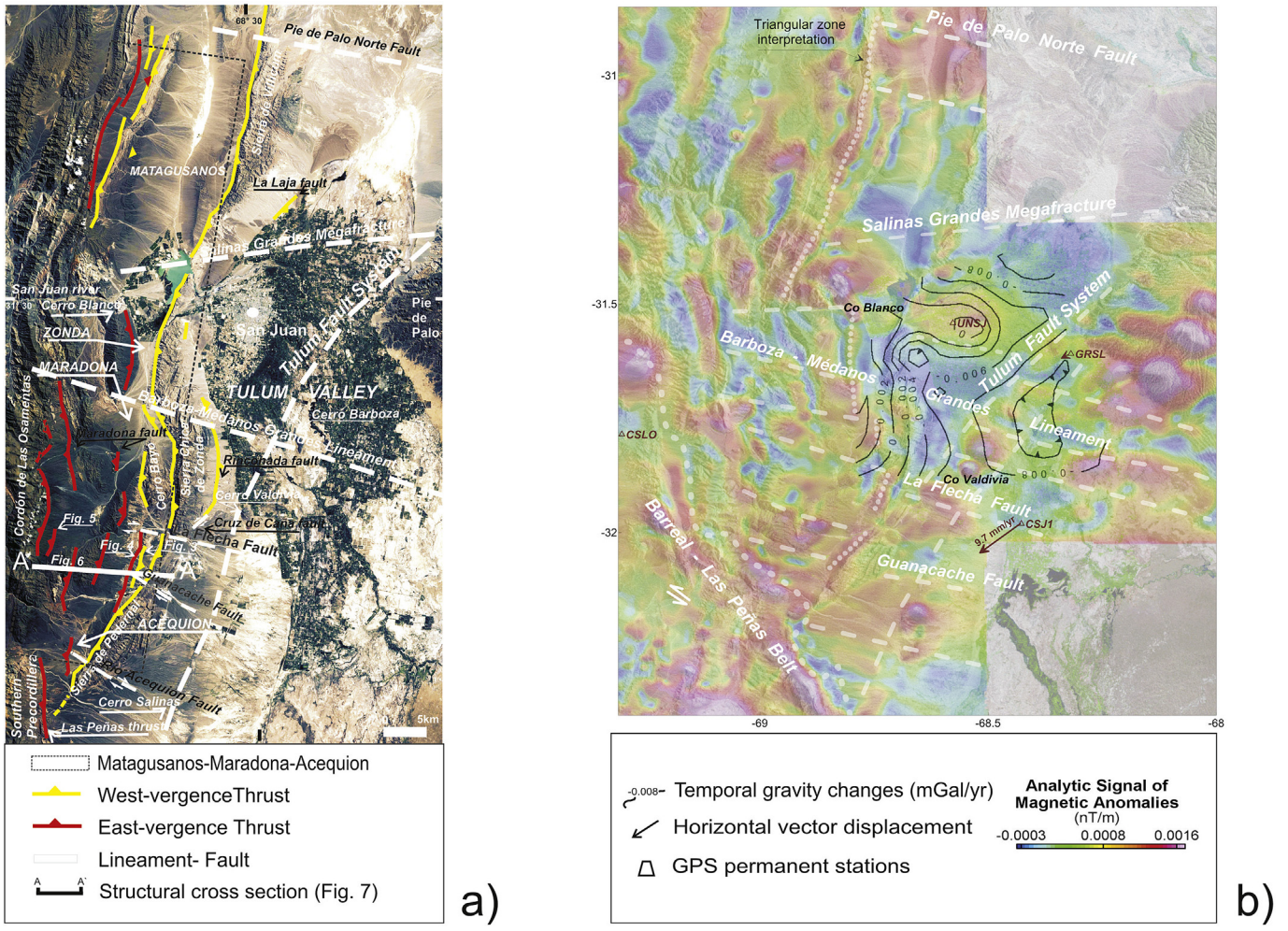

Fig. 2. (a) Landsat TM image centered on the study area (Matagusanos-Maradona-Acequión corridor). Main west-vergence and east-vergence Quaternary faults and main E–W lineaments were indicated. (b) Analytic signal map of total magnetic anomalies upward continued to 1.5 km altitude and structural interpretation (white). Brown vector: differential horizontal GPS velocity (CSJ1-CSLO).

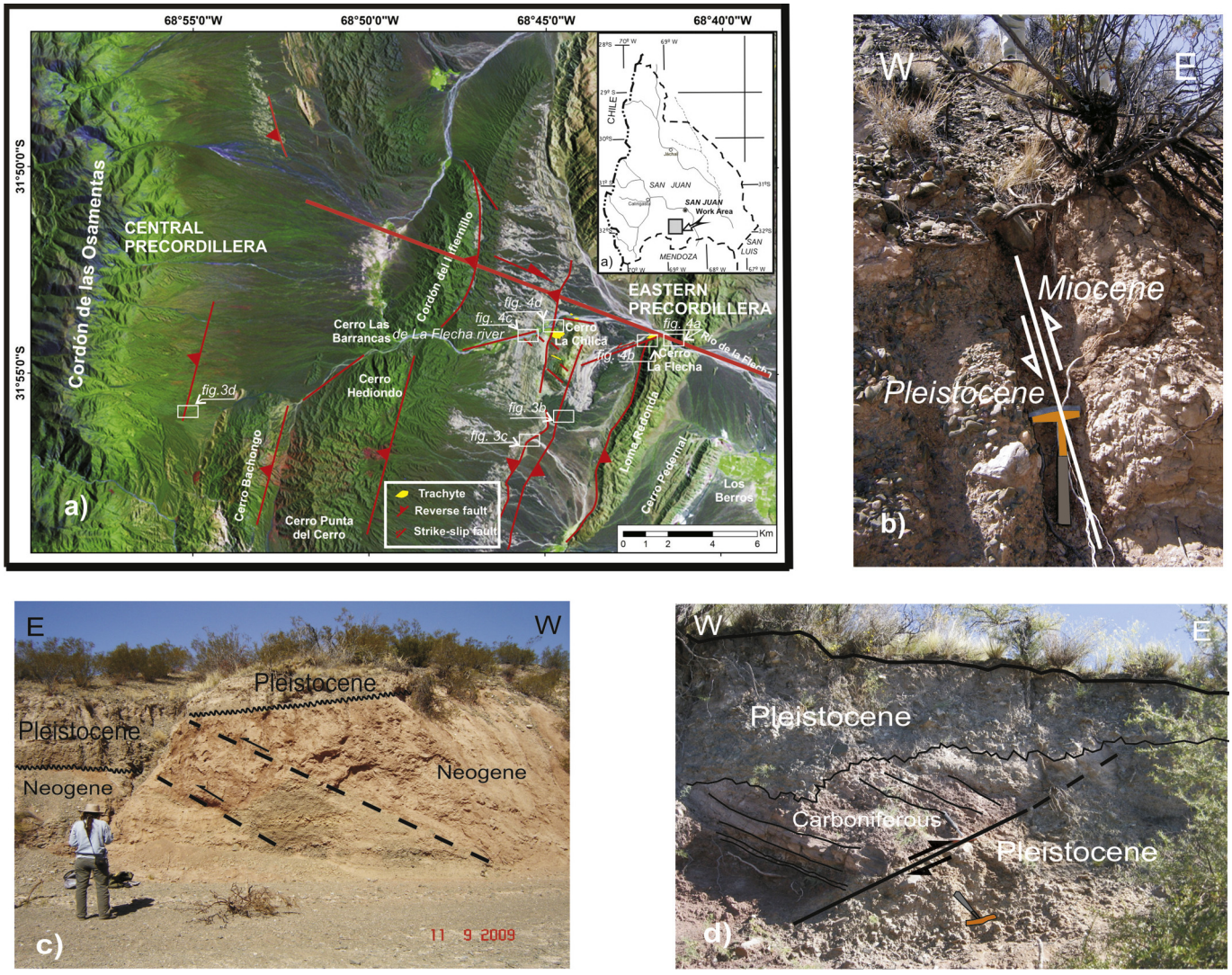

Fig. 3. (a) Satellite image centered on the study area and field photographs location. Field photographs showing: (b) trench located in the north portion of El Mocho fault, showing Miocene sediments which have been thrusted onto Pleistocene fanglomerates dipping 70°E, (c) exposure of Cerro La Chilca fault that dips 25°–30° W, showing Pleistocene fanglomerates underlying Neogene bedrock and (d) exposure of a thrust fault that dips 30°W and puts Carboniferous rocks over Pleistocene fanglomerates.

structure developed as a consequence of gradual flattening of the Nazca Plate in the last 20 Ma. The authors interpreted that its orientation and complex structural geometry are a result of the interference of the Late Cenozoic Andean deformation with the NW-trending rift structure of the Triassic Cuyo basin and the ancient collisional suture zones of Paleozoic age. The belt is formed by partially overlapping faulted mountainous blocks with a left-stepping array. They recognize blocks bounded by reverse faults with an azimuth ~160° to N–S of both East and West vergence and oblique sinistral faults (azimuth ~140°). The association of thrust and strike-slip faults, the stepped arrangement and their oblique orientation to expected regional efforts in plate convergence direction, helped these authors to interpret a transpressive character for the region. Fazzito et al. (2009) mentioned that the Southern Precordillera has evolved under the influence of structural anisotropies as oblique mega-shear zones with NW trending and paleogeographic features of Paleozoic and Triassic age (Cortés et al., 2005, 2006).

Giambiagi et al. (2011) made a detailed investigation of the structure and evolution of the Precordillera southern sector (South of 32°S) and described a west verging style characterized by partitioned transpression with a high shortening component, and an oblique strike-slip dominated subdomain. They concluded that the Cambrian–Quaternary units of the Precordillera at this latitude contain complex patterns of both superimposed and reactivated structures.

2.1. Neotectonic structures between La Flecha and Guanacache faults

Rolleri (1969) described the Matagusanos valley as a compressional graben that continues to the south between the eastern rims of the outer most range of the Eastern Precordillera and the fault which passes along the western flank of cerros Valdivia and Salinas (Tulum Fault?), (Fig. 2a). However, Perucca (1990) called Matagusanos-Maradona-Acequión corridor to a tectonic depression elongated N to NNE. That depression is situated between the morphostructural units Central Precordillera to the west and Eastern Precordillera to the east (Fig. 2a). This tectonic corridor separates two different structural domains: an eastern west-vergent one, where reverse faults show west facing scarps, and a western east-vergent domain, where scarps face west (Perucca,

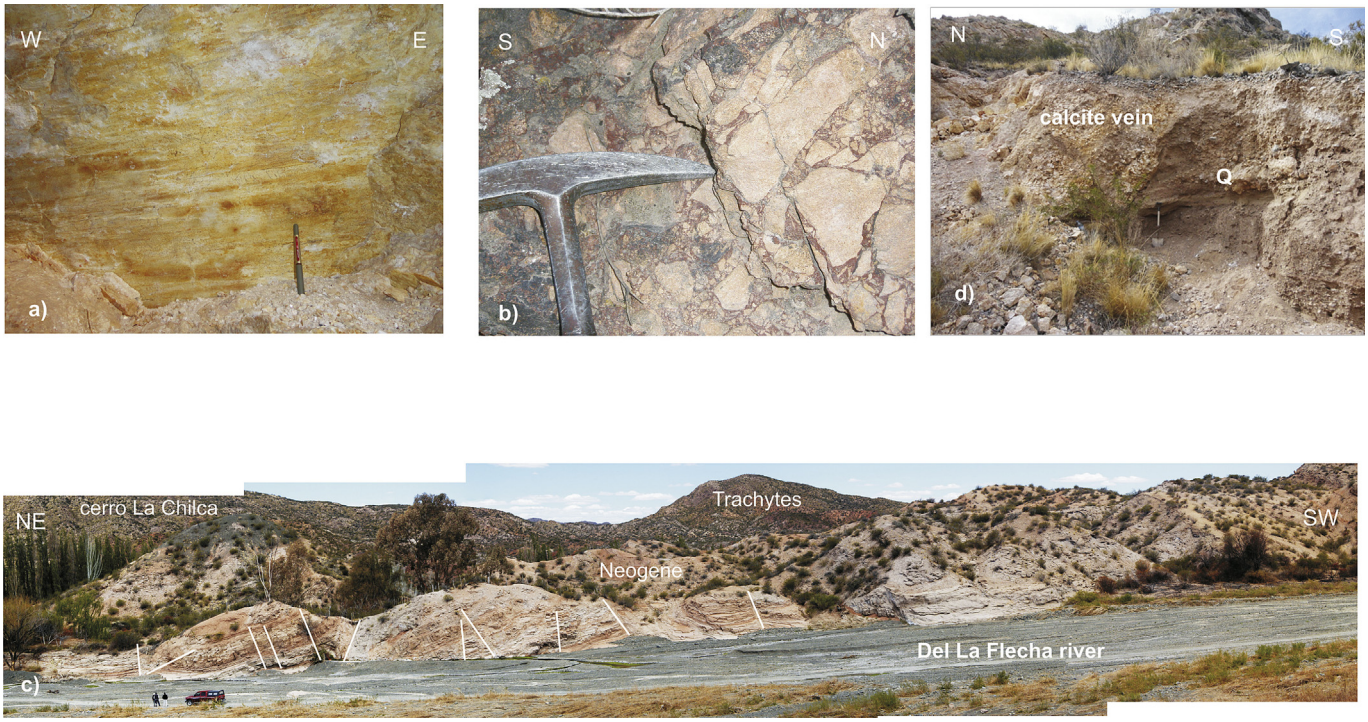

Fig. 4. (a) W–E calcite-filled veins with horizontal striae, (b) W–E brecciated trachyte dykes showing post-triassic activity of the fault (b) Fault trending E–W and showing a vein of post ordovician calcite over Quaternary deposits, (c) faults trending E–W and affecting neogene rocks, and (d) fault trending E–W showing a vein of Paleozoic calcite over Quaternary alluvial deposits.

1990; Siame et al., 2006). Virtually most of the Quaternary deformation in the area is characterized at the surface by reverse faulting parallel to bedding.

To the north, in the Matagusanos depression (Fig. 2a), Costa et al. (1999) observed sub-parallel reverse faults with west vergence and high dip angles close to the surface in the western flank of Precordillera Central. These authors stated that these structures could be the result of displacements between bedding planes. Paredes and Perucca (2000) made a detailed analysis and fieldwork of the Quaternary faults of the western portion of the depression and interpreted that these structural changes in vergence take place at least 1.5 km east of the Central Precordillera ranges.

Gardini (1993) developed a balanced structural section of the Zonda valley south of the San Juan River (Fig. 2a). He interpreted deep regional structures affecting the basement to the east, beneath the sierra Chica de Zonda (Eastern Precordillera) and structures to the west closer to the surface in the Central Precordillera (Fig. 2a) outlining a triangular zone in a transverse section to the Precordillera between the Eastern and Central Precordillera.

Several authors (Amos, 1954; Amos et al., 1981; Perucca, 1990; Perucca et al., 1990; Moreiras and Banchig, 2008; Perucca and Onorato, 2011) carried out studies in the eastern piedmont of the Central Precordillera, and recognized east-verging reverse faults situated north of the study area. South of the Del Agua River (Fig. 1a), Giampaoli and Cegarra (2003) interpreted that the regional structure in this area consists of an imbricated sequence of fault propagation folds and out of sequence thrusts related to the uplift of the Eastern Precordillera, with a main detachment level near the top of the Cambro-Ordovician deposits.

South of 32°S, Ahumada and Costa (2009) and Ahumada (2010) identified the end of the triangular zone in the region where the Eastern, Central and Southern Precordillera interact. They state that Quaternary deformations north of the 32°S are predominantly expressed by west-vergence, NNE striking thrusts, belonging to the Eastern Precordillera. South of this latitude, thrusts are predominantly east-vergent and strike NNW, related to the Southern Precordillera (Fig. 2a). According to these authors, this structural arrangement determines an interaction of the antithetic overthrusts, in which the Quaternary displacement is transferred from one system to the other (Ahumada, 2010).

In our study, two areas with opposite vergence of Quaternary faulting were analyzed between La Flecha and del Agua rivers. The first one is located, in the eastern portion of the depression and SE of the cerro La Chilca, in the so called El Mocho fan (Uliarte et al., 1987) (Fig. 3a and b). The second area to the west is situated south of the cerro La Chilca (Fig. 3c) in the eastern piedmont of the Las Osamentas range (Fig. 3d). In the El Mocho fan, five faults with Quaternary activity are characterized by their straight traces and parallelism. Their scarps face against the runoff, and fault planes affecting this alluvial landform coincide with the bedding of the Neogene sedimentary rocks, trending N20°E. These faults are west verging, with high dips (>60°). Four of these faults affect only the oldest alluvial level (Pleistocene) but the main fault in its southern prolongation disturbs younger deposits (Pleistocene-Holocene age). This fault continues further to the north, trending N–S and affecting Neogene (Miocene) rocks (Fig. 3a).

The main fault, called El Mocho, is an N20°E striking fault that dips 70°E in average, but locally shows values nearing 80°E (Fig. 3a and b). At surface, this structure affects Miocene rocks, which have been thrusted onto Pleistocene conglomerates. The scarp, which reaches 18 m in height is subdued and rounded, indicating possible absence of Holocene reactivations. The trace prolongs south beyond the El Mocho fan (Perucca and Onorato, 2011).

The Cerro La Chilca fault is located few meters west of the El Mocho fault (Fig. 3c). It is 11 km long and strikes N15°E, south of the La Flecha River. Situated in the depression between the Cerro Bachongo and Punta del Cerro in the west and the Loma Redonda in the east, close to the La Chilca cattle station, it extends as far south as the Del Agua River. La Chilca is a reverse fault that dips 25°–

30°W and superimposes Neogene sedimentary rocks on Pleistocene alluvial levels (Perucca and Onorato, 2011).

Reverse faults with Quaternary tectonic activity are also found (Fig. 3d) in the eastern piedmont of the Cordón de Las Osamentas that is in the Central Precordillera and in the western sector of the Bachongo plain (31°45′S and 68° 55′W). This piedmont covers a much greater area than the Eastern Precordillera piedmont, due to the greater dimension of its hydrographic basin (Fig. 1a). Two generations of Quaternary alluvial fans and a current accumulation level produced by channel fill were identified in this eastern piedmont. The thickness of the Quaternary alluvial cover varies from 30 m in the apical-middle sector to 10 m in the distal zone (Perucca and Onorato, 2011). Within the study area the fanglomerate alluvial cover, which is strongly incised, lies upon Carboniferous (Harrington, 1971) and Neogene (Leveratto, 1968) sedimentary rocks. N–S trending thrust faults affect the lower or distal part of the alluvial fans; east-facing scarps up to 10 m high underline the fault trace. The westernmost fault in the study area, named Las Osamentas fault by Perucca and Onorato (2011), has a 350° azimuth and dips 30° west. It displaces Carboniferous deposits over Pleistocene sedimentary rocks with strong dips (Fig. 3a and d). No field evidence has been found proving any tectonic activity on the Holocene units. This could suggest a lower tectonic activity for the region during the upper Pleistocene and Holocene.

In addition, Ruiz et al. (2011b) have shown gravity time variations (4D gravity) produced by ongoing tectonic activity from a geodetic network extended over an area of 3500 km^2 centered on San Juan City. These gravity changes obtained during the years 2000–2009 from periodic gravity measurements support the current uplift of the Eastern Precordillera. The authors identify three segments with higher activity: (a) La Laja fault with strong decreases of gravity, (b) Maradona-Cerro Bayo segment, with increases of gravity westwards of the Sierra Chica de Zonda, and (c) decreases of gravity at La Rinconada fault. The data show tectonic activity in the Tulum fault system and gravity changes that are consistent with the Cerro Valdivia–Cerro Barboza–Sierra Pie de Palo lineament and increased to the east (Fig. 2b). The largest gravity variations are observed eastwards of Cerro Barboza with a minimum of gravity changes.

3. Geophysical methods

The present study is based on gravity and magnetic anomalies from the Instituto Geofísico Sismológico (IGSV), Universidad Nacional de San Juan database.

Terrain corrected Bouguer anomalies were calculated from 5000 gravity stations collected by IGSV (Ruiz and Introcaso, 2004; Ruiz et al., 2011b). The total field magnetic anomaly mosaic was prepared by merging data from two aeromagnetic surveys (SEGEMAR, 1999, 2001). The merged grid was controlled and leveled by means of terrestrial magnetic data (Ruiz et al., 2011a).

3.1. Analytic signal of magnetic anomalies

In this paper, the total magnetic gradient (analytic signal) of magnetic anomalies has been used to enhance anomalies of tectonic interest and to obtain some preliminary information on source location and magnetization distribution. The use of analytic signal amplitude (Nabighian, 1972) allows for the geophysical prospecting in low magnetic latitudes. Conveniently, the amplitude peaks exactly at the edge of the buried dipping contact causing the magnetic anomaly (Nabighian, 1972; Roest et al., 1992; Nabighian et al., 2005). The analytic signal is independent of inclination, declination, remaining magnetization and dip, when the magnetic sources are 2D (Blakely, 1995). The only disadvantage is that the analytic signal anomalies are relatively much broader than the lateral extent of the buried target.

To identify the possible subsurface geological structure within the study area, the total field magnetic anomaly data needs to be upward continued to 1.5 km before the total magnetic gradient amplitude is calculated (Fig. 2b). A cursory examination of the magnetic map reveals the following structural patterns.

(1) The magnetic fabric of Central and Eastern Precordillera shows a sigmoid geometry with regional N–S trending. The long-wavelength band is dominated by low-amplitude features (cold colors). In the southwestern region, this pattern converges sharply in a linear crest (hot colors) trending NNW, coinciding with the beginning of the Southern Precordillera (Barreal-Las Peñas Belt).
(2) The Pie de Palo-Precordillera magnetic contact appears as a semi-linear anomaly pattern trending NE from the north of Southern Precordillera to the western Pie de Palo range (Tulum fault system). There is an evident contrast in magnetic fabric across the contact line. To the east, the Pie de Palo buried basement is dominated by trending lineaments parallel to the contact (NE) and transverse to it (NW). At least the first 10 km of the magnetic belt stretching from the outcrops of western Pie de Palo range to the Cerro Valdivia, have the same magnetic characteristics.
(3) The limestone rocks of the Eastern Precordillera produce low-amplitude analytic signal. The same pattern is shown in the Tulum Valley basin, except for a maximum possibly representing a local high of basement below San Juan City. These anomalies consist of long wavelength and come from deeper sources (basement sources). The San Juan City basement block has high vertical crustal mobility, the boundaries of which agree with three 4D gravimetric gradients of about −0.005 mGal/yr (Ruiz et al., 2011b). The contour lines of gravity time variations in are show in Fig. 2b.
(4) The analytic signal map reveals regional lineaments running transversal to the orogenic front: (a) Salinas Grandes Megafracture, (b) Barboza-Médanos Grandes lineament (Ruiz et al., 2011b), (c) La Flecha fault, (d) Guanacache fault, (e) Acequión Fault and (f) Barreal-Las Peñas Belt. These transversal lineaments show displacements in its trend through the Precordillera–Pie de Palo contact, inferred from the anomaly patterns.
(5) Short-wavelengths of maxima (hot colors) are related to rocks with high content of magnetite (crystalline rocks, red sediments). These magnetic highs delineate: (a) the Cerro Blanco pluton, (b) the Sierra Pie de Palo ophiolitic complex (Vujovich, 2003), (c) Cerro Valdivia and Cerro Salinas, (d) Carboniferous and Neogene deposits and (e) possible minor intrusive subsurficial bodies.

Ruiz et al. (2011b) using 4D gravity data combined with gravity and magnetic anomalies analysis have shown the existence of a conspicuous lineament of maxima that connects the western margin of Sierra Pie de Palo with Barboza and Valdivia hills and converging to the Eastern Precordillera at the latitude of La Flecha River. This lineament is the geophysical evidence of the Tulum fault system, with Quaternary tectonic activity which represents a basement structural high, buried bellow the Tulum basin. This structure coincides with the contact (Pattern 2) analyzed in this paper (Fig. 2b) and is highly correlated with more superficial interpretation of Zambrano and Suvires (2008).

We interpret the magnetic contact between Precordillera and Pie de Palo as an oblique coupling at the basement level of the Caucete Group with meta-sedimentary rocks outcropping at the

western slope of Sierra de Pie de Palo (Vujovich, 2003) as part of Pie de Palo basement against Precordillera basement. Since faulting in shallower sections is often controlled by reactivation of basement faults, it is possible to expect that the modern shallow structures reflect the basement fabric (Fig. 5). The oblique coupling of these terranes with possible differential strain transfers could generate structural complexities which could partly explain the sigmoidal geometry of Eastern Precordillera and, by reactivation of ancient basement structures, the faults transversal to the regional thrust.

In the last four years, four permanent GPS stations have been installed in the area under study. Preliminary geodetic velocity field reveals that the northern velocity component of Precordillera is slightly greater than Western Sierras Pampeanas velocity (IGN, 2013). By calculating the horizontal vector difference between CSJ1 (31°59'S, 68°26'W) and CSLO (31°45'S, 69°18'W) GPS stations during the 2010–2012 records, we find 9.7 mm/yr, Azimuth 234° (Fig. 2b). Temporary GPS data of Klotz et al. (2001) close to both permanent stations allowed us to obtain 7.9 mm/yr, Azimuth 226°. Part of this deformation (~5.0 mm/yr, Az 240°, obtained from stations located at both edges of Precordillera (Brooks et al., 2003)) has been accommodated within the Precordillera (Siame et al., 2006). The remnant SW directed dextral slip of ~4.5 mm/yr, reinforces the idea of oblique basements convergence with strain partially absorbed by transcurrent deformation and shortening, deflecting the Eastern Precordillera westward.

The main magnetic lineaments, transverse to the direction of the orogen are shown in Fig. 2b. These lineaments show a dextral displacement on both sides of Tulum fault system. Furthermore, based on the Analytic Signal map and surface geological evidence, we have identified the location of the triangular zone, associated in our interpretation to a high in the basement that has been highlighted by the second derivative of the Analytic Signal (Fig. 5) and can be followed throughout the map. This high is also observed in the Matagusanos-Maradona-Acequión valley as a linear maximum with NS direction laterally offset by transverse lineaments.

3.2. Gravi-magnetometric inversion model

In order to make a gravi-magnetometric model of the area separating the oppositely verging thrust systems of Precordillera, we analyzed the total field magnetic anomalies and residual Bouguer anomalies in an E–W section, crosscutting the triangular zone (Fig. 5).

Werner deconvolutions (red symbols) and Analytic Signal contact depth solutions (black symbols) were carried out from the magnetic field along the profile (Fig. 5). The solutions were computed using PDEPTH software (Phillips, 2007). The Werner deconvolutions and analytic signal (Nabighian et al., 2005) methods for magnetic profiles have been widely used as part of an automated interpretation routine system (Hartman et al., 1971; Ku and Sharp, 1983; Tsokas and Hansen, 1996; Nabighian et al., 2005; Gimenez et al., 2009; Ruiz and Introcaso, 2011). Assuming hypothetical source geometry, the Werner-based deconvolution of the recorded field yields a two-dimensional geological source distribution and an associated magnetic parameter distribution: Werner's depths, horizontal locations, dip angles, and magnetic susceptibility contrasts (Blakely, 1995). The Werner horizontal gradient solution is a good indicator of the edge of a thick interface body (contact). The use of these types of solutions leads to a close approximation to depth estimation, and reveal the geometry of the different magnetic bodies.

Sweeping the deconvolution operator along the magnetic field profile, different series of solutions can be estimated (Fig. 5). Depths are indicated by crosses, orientation vectors are indicated with the same dip angles of each solution (dip angle of the body interface with 90° ambiguity) and susceptibility contrasts proportional to the vector size (Fig. 5). Contact solutions on the profile have been analyzed, the foreland basin structural style has been identified and major structures have been recognized, in particular the depth to basement and edges of clastic continental (reddish) rock units.

Werner solutions are grouped into faults and strata layers. We have interpreted a system of faults dipping to the east beneath the Eastern Precordillera outcrops. Immediately to the west of this structure, east-verging basement faults are interpreted. This is a magnetic evidence of the tectonic triangular zone involving the crystalline basement.

Residual decompensative gravity anomalies (Ruiz et al., 2011b) have been used to calculate the inversion model. A two-step process to isolate the upper crust signal from the gravity anomalies was applied. First, an isostatic residual anomaly map was generated by removing the gravity resulting from a modeled crustal root of topography from the Bouguer anomalies, assuming Airy isostasy (purely local compensation). Decompensative correction includes removing the gravity contribution of the crustal compensation for the geological load from the isostatic residual anomaly, to yield the

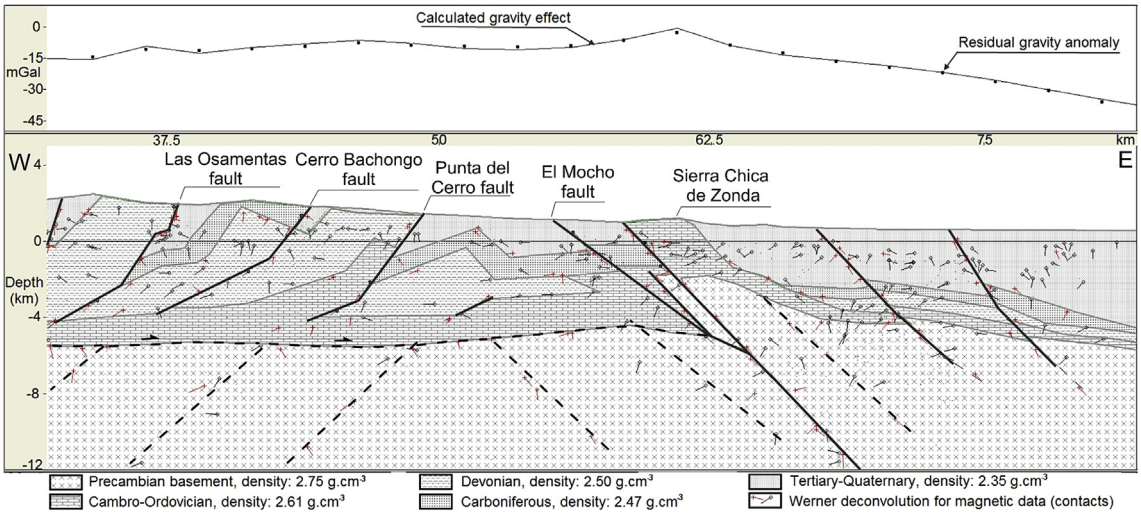

Fig. 5. Balanced structural cross-section calculated by 2D gravimetric inversion adjusted with Werner (red symbols) and analytic signal (black symbols) solutions. Top: calculated anomaly (line) and residual anomaly (broken line). Bottom: crustal model. (For interpretation of the references to color in this figure legend, the reader is referred to the web version of this article.)

decompensative anomaly (Cordell et al., 1991). We have approximated this correction by extending the isostatic anomaly upwards by 35 km to filter out the upper- and mid-crust gravity contributions (Ruiz et al., 2011b).

The 2D gravity model was adjusted by the magnetic contact distribution, and the structurally balanced cross-section based on a seismic section located 10 km to the south (Giampaoli and Cegarra, 2003). The mean depth to the basement has been obtained in the frequency domain from the logarithmic graph of the radially averaged power spectrum versus wavenumber of the gravity and magnetic anomalies (Blakely, 1995). The long wavelengths of both Bouguer and magnetic anomalíes have been analyzed in 65 km wide square windows (with the modeled cross-section in the center). By fitting a straight line through the high-wavenumber part of the spectrum we calculated a 5.2 km depth to the magnetic basement and a 5.9 km mean depth to the gravity basement (Fig. 6).

In the gravity inversion model, the well known 2D GM-SYS software based on Parker's algorithm (Parker, 1972) was used. We computed a model of five layers: topography (with lateral variation of density obtained from outcrops); Neogene–Quaternary layers with a mean density of 2.35 g cm^{-3}; Carboniferous deposits with a mean density of 2.47 g cm^{-3}; Devonian with a mean density of 2.50 g cm^{-3}; Cambro-Ordovician layers with a mean density of 2.61 g cm^{-3}; and a basement density of 2.75 g cm^{-3} (Table 1). The layer densities were computed from sonic logs from Matagusanos and Las Peñas oil exploration wells (YPF, 1961, 1981, 1985). Both wells are located no more than 70 km of the modeled gravity section. By means of Gardner's velocity–density relations (Brocher, 2005) we calculated the weighted average density of each layer. The resulting model demonstrates that the basement crystalline geometry and the most important structures of the upper crust can be interpreted using this approach. The error between calculated and observed anomalies in this case is very small (about 2.07%).

Faults were inferred from deconvolutions, considering the surface geology. The most conspicuous result of the study is the tectonic wedge facing the two vergences which was modeled as a high on the faulted basement folding the younger sediments. Here, the fold-thrust belt detachment is present in the lower Ordovician shale. The model interpretation shows the influence of basement structures in the change of vergences and the anomalous position of the wedge, which runs toward the axis of the Zonda regional fault south of the Quebrada de La Flecha. The main control of these previous structures corresponds to the location of ramps in the basement along which deep detachment thrusts propagating toward the Quaternary sedimentary cover.

Table 1
Mean density from exploration wells on Tulum and Matagusanos valleys. Wells of YPF: YPF-SJMA-1 (1961), YPF-SJ-M-es-1 (1981), YPF-SJ-SP-es-1 (1985).

Mean density from hydrocarbon exploration	
Layers	Density g cm^{-3}
Neogene–Quaternary	2.35
Carboniferous	2.47
Devonian	2.50
Cambro-Ordovician	2.61
Cristalline basement	2.75

4. Discussion

The interpretation of the data centered in the area between the La Flecha and Del Agua rivers produced the following results:

In the eastern edge of the depression, the Zonda regional fault uplifted the Loma Redonda limestone range, where geomorphic evidence (drainage patterns anomalies and several different alluvial levels) suggests Quaternary tectonic activity (Fig. 3a). This west-vergence thrust is deeply rooted affecting the basement by bringing it close to the surface (Comínguez and Ramos, 1991; Von Gosen, 1992) as it is shown in our inversion geophysical model (Fig. 6). The faults observed in the El Mocho fan area and in its southern prolongation, between the La Flecha and Del Agua rivers, show similar characteristics to those described in Matagusanos by Paredes et al. (1996), Costa et al. (1999) and Paredes and Perucca (2000). They are sub-parallel reverse faults with high angle at the surface dipping to the east, in coincidence with the Neogene sedimentary rocks bedding, highlighted by a peak of maxima in the analytic signal map (Fig. 2b).

In the Central Precordillera, conversely, the Cordón de Las Osamentas is characterized by an east mountain front elevated by an east-vergence thrust, whose plane is inclined between 20 and 50°W. This mountain front has a marked rectilinear trace and shows faceted spurs, indicative of Quaternary tectonic activity. Other faults in this region, as the Las Osamentas thrust and those affecting the Cordón del Infiernillo and the Cerro Bachongo in the east, have east vergence too.

Jordan et al. (1983a) pointed that one of the questions that must be answered to understand the role of plate tectonics in deforming continents concerned the extent of inherited structures such as faults predetermining and controlling location of structural province boundaries.

Milana (1990) pointed that Pie de Palo Norte lineament (Fig. 2) bounds the northern end of the sierra de Pie de Palo and crosses the

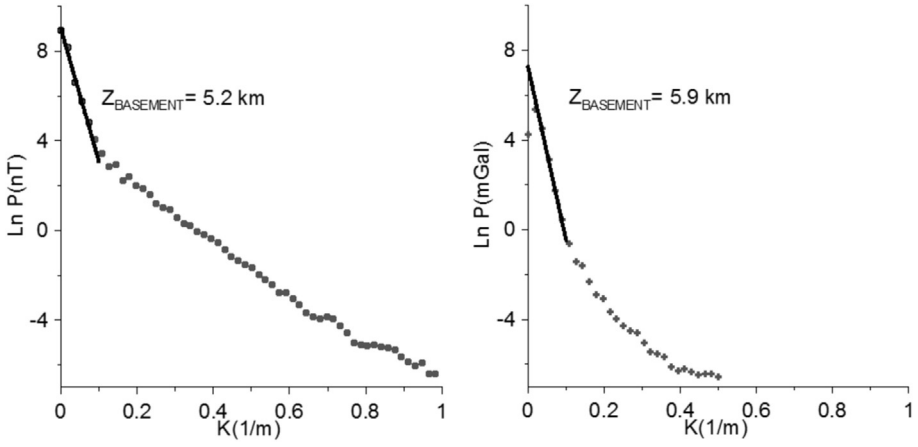

Fig. 6. Spectral depth estimates for the Precordillera basement from the logarithmic radial average power spectrum (ln P) as a function of wavenumber (*K*), window length 65 km centered in El Mocho fan (Fig. 2c). Estimated mean depths to the top of the basement: Left: fitting straight line through high *K* of total magnetic anomalies; right: from Bouguer anomalies.

Eastern Precordillera where it causes left-lateral offsets of Tertiary units. Zapata and Allmendinger (1996a,b) and Zapata (1998) considered that this sinistral fault may either branch off the Eastern Precordillera decollement or cut deeper into de crust.

Paredes and Perucca (2000) indicated an eastward shift of the triangular zone axis in the Matagusanos depression, bounded by the Pie de Palo Norte Fault, and the Salinas Grandes mega-fracture on the north and south, respectively (Fig. 2).

Siame et al. (2002, 2006) recognized that north of 31°S, the Eastern Precordillera is characterized by thick-skinned, blind thrusts and folds developed within the Neogene strata of the Bermejo valley, whereas it is marked to the south by thick-skinned emergent thrusts carrying mostly Paleozoic rocks. These authors concluded that the location of this change in the structural style of the Eastern Precordillera coincides with the north Pie de Palo Fault, which trends WSW (Fig. 2a). Therefore, the change of the triangle zone axis defined by the Central and Eastern Precordillera interaction in this area may be partially influenced by the Sierras Pampeanas active broken-foreland. The authors concluded that the Andean back-arc of western Argentina can be regarded as an obliquely converging foreland where Plio-Quaternary deformations are partitioned between strike-slip and thrust motions. These strike-slip and thrust motions are localized on the east-verging thin-skinned Argentine Precordillera and the west-verging thick-skinned Sierras Pampeanas, respectively.

We are proposing a similar condition for the region between the La Flecha and Del Agua rivers, but with a more moderate jump. This could have been caused by a faster advancement to the west of a Paleozoic basement block that would have been limited to the north by the La Flecha fault and to the south by the Guanacache fault. The la Flecha fault dextrally offsets about 1 km the Sierra Chica de Zonda front in relation to the Loma Redonda mountain front, and almost 400 m to the Plio-Pleistocene deposits upstream of La Flecha River.

From well data and electric resistivity surveys, Zambrano et al. (2005) proved that the La Flecha fault continues several km to the SE into the subsurface of the Tulum valley and that the Guanacache fault, parallel to the La Flecha fault, coincides rather well with the Del Agua River course. The authors noted that the Guanacache fault continues to the SE in the subsurface of the Tulum valley affecting Quaternary deposits (Fig. 2). These faults trend more or less transverse to the N–S system. Probably those faults oriented WNW have had diverse strike slip values, as it seems to be shown in the surface and the subsurface structures and on our results in the analytic signal map.

Fieldwork focused in the Del Agua Creek showed a reverse fault affecting Carboniferous sedimentary rocks with a 275° azimuth, which dips 87° to the north (Guanacache fault). Horizontal striae on the fault plane (pitch 0°) support a strike-slip component. Although it is unclear whether the fault directly affects Quaternary deposits, it does control the drainage pattern in this area.

According to Ruiz et al. (2011b) the Caucete Group, as part of the Pie de Palo basement, is related with a high of the basement buried beneath Tulum basin. This lineament is named the Tulum fault system (Zambrano and Suvires, 2008) and has evidence of high tectonic activity with a topographic uplift of more than ~10 cm in the last ten years. By the analytic signal evidence, the Tulum fault system (Fig. 2b) shows a conspicuous rectilinear lineament that suggests an oblique coupling between both the Eastern Precordillera thrust and Western Sierras Pampeanas basement. This structural complex interaction could generate a high seismic activity (i.e. La Rinconada 1952, 6.8 Mw earthquake) by stress transfer between both terranes in a regional thrust regime, generating reactivation of pre-Neogene transverse faults.

Eastern Precordillera interacts at La Flecha and del Agua rivers latitude with the Tulum dextral strike-slip fault system (SW ~4.5 mm/yr horizontal GPS velocity), involving basement. This oblique basement convergence could have generated small rotations in areas of basement weakness. It could have also generated the shortening and the sigmoidal geometry of the fold-and-thrust belts of Sierra Chica de Zonda and Pedernal ranges. Both buried basement systems converge and strike with the Southern Precordillera at 32°10′S, generating stress transfer and favoring the reactivation of Triassic transcurrent NW structures such as that described by Cortés et al. (2006) for the Barreal-Las Peñas belt.

The modeled cross-section shows the influence of basement faults in the location of the tectonic wedge, in the form of a high on the basement which would propagate toward the Quaternary sedimentary cover.

5. Summary and conclusions

Neotectonic features between the La Flecha and Del Agua rivers include several fault traces, developed within Quaternary deposits, which are the result of the interaction of two morphostructural fronts with opposite vergence. The west-vergence blocks of Eastern Precordillera would have produced NNE-trending reverse faults with the footwalls toward the west (El Mocho and parallel thrusts), whereas the Central Precordillera thrust belt would have generated NNE-trending reverse faults with downthrown blocks to the east (Las Osamentas and La Chilca thrusts). Some E–W trending faults show evidence of neotectonic activity, like the Cruz de Caña and La Flecha faults. Analysis of recent structural data supports the argument of basement-involved tectonics on the foreland fold-and-thrust belt whereas new geophysical work supports the thick-skinned model for the Eastern Precordillera thrust belt. We have therefore distinguished areas where prominent shallow deformation occurs (Central Precordillera) and those where basement involvement dominates (Eastern Precordillera). In the studied area, neotectonic activity is focused along Pampean-type thrusts, which constitute the reactivation of the Sierras Pampeanas fabric, where the orogenic front was displaced into its current position.

The change in the position of the triangle zone axis from N to S, alternating to the east or the west along the Matagusanos-Maradona-Acequión tectonic corridor, would have taken place during the Quaternary and would possibly have been related to transversal structures and to the Pie de Palo mountain range. These inherited features could be explained by geodetic and geophysical evidences of the oblique contact between the Eastern Precordillera and the Pie de Palo basements. The stress transfer must have generated significant neotectonic activity as the measurement of gravity temporal changes related with uplift of Tulum faults system reveals. These transversal lineaments would have exerted a strong control on the structural segmentation of Quaternary tectonic activity along the north–south mountain fronts of Central and Eastern Precordillera.

Finally, this overall geometric framework provides new insights about a classic area, illustrated by several field evidences and geophysical and geodetic data.

Acknowledgments

The authors especially thank the reviewers for their helpful comments. Special thanks to R. Onorato, N. Vargas, M. Rothis and E. Luna for their helpful assistance during fieldwork. Finally, the authors acknowledge funding received from PID 0799 of Consejo Nacional de Investigaciones Científicas y Técnicas (CONICET), PICTO 2009-UNSJ-0013 and CICITCA 21E905 and 21E870 to support this research.

References

Ahumada, E., 2010. Neotectónica del Frente Orogénico Andino entre los 32° 08′ S–32°19′S, provincias de Mendoza y San Juan. Unpublished PhD thesis. Universidad Nacional de San Luis, p. 155.

Ahumada, E., Costa, C., 2009. Antithetic linkage between oblique Quaternary thrusts at the Andean front, Argentine Precordillera. J. South Am. Earth Sci. 28 (3), 207–216.

Allmendinger, R., Figueroa, D., Snyder, D., Beer, J., Mpodozis, C., Isacks, B., 1990. Foreland shortening and crustal balancing in the Andes at 30°S latitude. Tectonics 9 (4), 789–809.

Alvarado, P., Pardo, M., Gilbert, H., Miranda, S., Anderson, M., Saez, M., Beck, S., 2009. Flat-slab subduction and crustal models for the seismically active Sierras Pampeanas region of Argentina. In: Kay, S., Ramos, V.A., Dickinson, W. (Eds.), MWR204: Backbone of the Americas: Shallow Subduction, Plateau Uplift, and Ridge and Terrane Collision. Geological Society of America, Boulder, Colorado, pp. 261–278.

Amos, A., 1954. Estructuras de las formaciones paleozoicas de la Rinconada, Pie Oriental de la sierra Chica de Zonda, San Juan. Rev. Asoc. Geol. Argent. 9 (1), 3–32.

Amos, J., Caligari, R., Siches, C., 1981. Las fallas activas en la República Argentina. In: 8° Congreso Geológico Argentino, 2, pp. 235–242.

Anderson, M., Alvarado, P., Zandt, G., Beck, S., 2007. Geometry and brittle deformation of the subducting Nazca Plate, Central Chile and Argentina. Geophys. J. Int. 171, 419–434.

Barazangi, M., Isacks, B.L., 1976. Spatial distribution of earthquakes and subduction of the Nazca plate beneath South America. Geology 4, 686–692.

Beck, S., Alvarado, P., Wagner, L., Anderson, M., Gilbert, H., Zandt, G., 2008. Flat-slab subduction beneath the Sierras Pampeanas in Argentina. In: Seventh International Symposium on Andean Geodynamics, pp. 75–76. Extended Abstracts.

Blakely, R., 1995. Potential Theory in Gravity and Magnetic Applications. Cambridge University Press, p. 441.

Brocher, T., 2005. Empirical relations between elastic wave speeds and density in the Earth's crust. Bull. Seismol. Soc. Am. 95 (6), 2081–2092.

Brooks, B., Bevis, M., Smalley, R., Kendrick, E., Manceda, R., Lauría, E., Maturana, R., Araujo, M., 2003. Crustal motion in the Southern Andes (26°–36°S): do the Andes behave like a microplate? Geochem. Geophys. Geosyst. 4, 1–14.

Castro de Machuca, B., Perucca, L., Conte-Grand, A., Pontoriero, S., Meissl, E., Martos, L., 2013. Edad y geoquímica del magmatismo traquítico de Precordillera Oriental, provincia de San Juan. In: Segundo Simposio sobre Petrología Ignea y Metalogénesis Asociada (CD-rom).

Comínguez, H., Ramos, V., 1991. La estructura profunda entre Precordillera y Sierras Pampeanas de la Argentina: Evidencia de la sísmica de reflexión profunda. Rev. Geol. Chile 18, 3–14.

Cordell, L., Zorin, Y.A., Keller, G., 1991. The decompensative gravity anomaly and deep structure of the region of the Rio Grande rift. J. Geophys. Res. 96, 6557–6568.

Cortés, J., Pasini, M., Yamin, G., 2005. Paleotectonic controls on the distribution of quaternary deformation in Southern Precordillera, Central Andes (31° 30–33° SL). In: International Symposium on Andean Geodynamics, pp. 186–189. Extended Abstracts.

Cortés, J., Casa, A., Pasini, M., Yamin, M., Terrizzano, C., 2006. Fajas oblicuas de deformación neotectónica en Precordillera y Cordillera Frontal (31° 30′–33° 30′ LS). Controles paleotectónicos. Rev. Asoc. Geol. Argent. 61 (4), 639–646.

Costa, C., Rockwell, T., Paredes, J., Gardini, C., 1999. Quaternary deformations and seismic hazard at the Andean orogenic Front (31°- 33°, Argentina): a paleoseismological perspective. In: Proceedings of the Fourth International Symposium on Andean Geodynamics, pp. 187–191.

Cristallini, E., Ramos, V., 2000. Thick-skinned and thin-skinned thrusting in La Ramada fold and thrust belt: crustal evolution of the High Andes of San Juan, Argentina (32° SL). Tectonophysics 317, 205–235.

Fazzito, S., Rapalini, A., Cortés, J., Terrizzano, C., 2009. Characterization of quaternary faults by electric resistivity tomography in the Andean Precordillera of Western Argentina. J. South Am. Earth Sci. 28, 217–228.

Figueroa, D., Ferraris, O., 1989. Estructura del margen oriental de la Precordillera Mendocina-Sanjuanina. In: 1° Congreso Nacional de Exploración de Hidrocarburos, 1, pp. 515–529.

Gardini, M., 1993. Estructura superficial y profunda del valle de Zonda, Precordillera de San Juan. In: 12° Congreso Geológico Argentino y 2° Congreso de Exploración de Hidrocarburos, 3, pp. 93–99.

Giambiagi, L., Mescua, J., Bechis, F., Martínez, A., Folguera, A., 2011. Pre-Andean deformation of the Precordillera southern sector, southern Central Andes. Geosphere, 1–21, 00572.

Giampaoli, P., Cegarra, M., 2003. Análisis estructural del extremo sur de la Precordillera Central Sanjuanina. Rev. Asoc. Geol. Argent. 58 (1), 49–60.

Gimenez, M., Martinez, M., Jordan, T.F., Ruiz, A., Introcaso, G., Bustos, Lince Klinger, F., 2009. Geophysical characterization of the La Rioja valley basin, Argentina. Geophysics 74 (3), B83–B94.

Harrington, H., 1971. Descripción geológica de la Hoja 22c, Ramblón, provincias de Mendoza y San Juan. In: Dirección Nacional de Geología y Minería, Boletín, vol. 114, pp. 1–81.

Hartman, R., Teskey, D., Friedberg, J., 1971. A system for rapid digital aeromagnetic interpretation. Geophysics 36, 891–918.

IGN (Instituto Geográfico Nacional), 2013. http://www.ign.gob.ar.

Jordan, T., Allmendinger, R., 1986. The sierras Pampeanas of Argentina – a modern analog of rocky-mountain foreland deformation. Am. J. Sci. 286, 737–764.

Jordan, T., Allmendinger, R., Damati, J., Drake, R., 1993. Chronology of motion in a complete thrust belt: the Precordillera, 30-31°S, Andes Mountains. J. Geol. 101, 137–158.

Jordan, T., Isacks, B., Ramos, V., Allmendinger, R., 1983a. Mountain building in the Central Andes. Episodes 3, 20–26.

Jordan, T., Isacks, B., Allmendinger, R., Brewer, J., Ramos, V., Ando, C., 1983b. Andean tectonics related to geometry of subducted Nazca plate. Geol. Soc. Am. 94 (3), 341–361.

Kendrick, E., Bevis, M., Smalley Jr., R., Brooks, B., Vargas, R., Lauría, E., Fortes, L., 2003. The Nazca-South America Euler vector and its rate of change. J. South Am. Earth Sci. 16, 125–131.

Klotz, J., Khazaradze, G., Angermann, D., Reigber, R., Perdomo, R., Cifuentes, O., 2001. Earthquake cycle dominates contemporary crustal deformation in the Central and Southern Andes. Earth Planet. Sci. Lett. 193, 437–446.

Ku, C., Sharp, J., 1983. Werner deconvolution for automated magnetic interpretation and its refinement using marquardt inverse modeling. Geophysics 48, 754–774.

Leveratto, M., 1968. Geología de la zona al oeste de Ullúm-Zonda, borde oriental de la Precordillera de San Juan, eruptividad subvolcánica y estructura. Rev. Asoc. Geol. Argent. 23 (2), 129–157.

Martinod, J., Husson, L., Roperch, P., Guillaume, B., Espurt, B., 2010. Horizontal subduction zones, convergence velocity and the building of the Andes. Earth Planet. Sci. Lett. 299, 299–309.

Martos, L.M., 1995. Análisis morfo-estructural de la faja pedemontana oriental de las sierras de Marquesado, Chica de Zonda y Pedernal: Su aplicación para prevenir riesgos geológicos: Provincia de San Juan. Unpublished Ph.D. thesis. Universidad Nacional de San Juan, p. 554.

Meigs, A., Krugh, W.C., Schiffman, C., Vergés, J., Ramos, V.A., 2006. Refolding of thin-skinned thrust sheets by active basement involved thrust faults in the Eastern Precordillera of western Argentina. Rev. Asoc. Geol. Argent. 61 (4), 589–660.

Milana, J.P., 1990. Sedimentología y magnetoestratigrafía de formaciones cenozoicas en el área de Mogna y su inserción en el marco tectosedimentario de la Precordillera Oriental. Unpublished PhD thesis. Universidad Nacional de San Juan, p. 273.

Moreiras, S., Banchig, A., 2008. Further evidences of quaternary activity of the Maradona faulting, Precordillera Central, Argentina. In: 7° International Symposium on Andean Geodynamics, pp. 344–347.

Nabighian, M., 1972. The analytic signal of two-dimensional magnetic bodies with polygonal cross-sections: its properties and use for automated anomaly interpretation. Geophysics 37, 507–517.

Nabighian, M.N., Grauch, V.J.S., Hansen, R.O., La Fehr, T.R., Li, Y., Peirce, J.W., Phillips, J.D., Ruder, M.E., 2005. The historical development of the magnetic method in exploration. Geophysics 70, 33–61.

Paredes, J., Perucca, L., 2000. Fallamiento cuaternario en la depresión de Matagusanos, San Juan, Argentina. Rev. Asoc. Geol. Argent. 55 (1–2), 23–30.

Paredes, J., Perucca, L., Tello, G., 1996. Fallas activas en el bolsón de Matagusanos, San Juan, Argentina. In: 12° Congreso Geológico de Bolivia, 3, pp. 1155–1163.

Parker, R.L., 1972. The rapid calculation of potential anomalies. J. R. Astron. Soc. 31, 447–455.

Perucca, L.P., 1990. Sistema de fallamiento La Dehesa-Maradona-Acequión, San Juan, Argentina. In: 11° Congreso Geológico Argentino, 2, pp. 431–434.

Perucca, L.P., Onorato, M.R., 2011. Fallas con actividad cuaternaria en el Corredor Tectónico Matagusanos –Maradona – Acequión entre los ríos de La Flecha y Del Agua. Provincia de San Juan. Rev. Asoc. Geol. Argent. 68 (1), 38–51.

Perucca, L., Sanches, A., Uliarte, E., 1990. Morfoneotectónica en la zona norte del corredor tectónico Matagusanos-Maradona-Acequión, San Juan, Argentina. In: 11° Congreso Geológico Argentino, 2, pp. 435–438.

Phillips, J., 2007. GeosofteXecutables (GX's). Developed by the U.S. Geological Survey, Version 2.0, with Notes on GX Development from Fortran Code. Open File Report 2007-1355, p. 111.

Pilger, R., 1981. Plate reconstructions, aseismic ridges, and low angle subduction beneath the Andes. Geol. Soc. Am. 92, 448–456.

Ramos, V., 1988. The tectonics of the Central Andes: 30° to 33° S latitude. In: Clark, S., Burchfield, D. (Eds.), Processes in Continental Lithospheric Deformation, Geological Society of America, Special Paper, vol. 218, pp. 31–54.

Ramos, V., Cristallini, E., Pérez, D., 2002. The Pampean flat-slab of the Central Andes. J. South Am. Earth Sci. 15, 59–78.

Ramos, V., Cegarra, M., Lo Forte, G., Comínguez, A., 1997. El frente orogénico de la sierra de Pedernal (San Juan, Argentina): su migración a través de los depósitos sinorogénicos. In: 8° Congreso Geológico Chileno, 3, pp. 1709–1713.

Roest, W., Verhoef, J., Pilkington, M., 1992. Magnetic interpretation using the 3D analytic signal. Geophysics 57, 116–125.

Rolleri, E., 1969. Rasgos tectónicos generales del valle de Matagusanos y de la zona entre San Juan y Jocoli, provincia de San Juan, República Argentina. Rev. Asoc. Geol. Argent. 24 (4), 408–412.

Rosenbaum, G., Mo, W., 2011. Tectonic and magmatic responses to the subduction of high bathymetric relief. Gondwana Res. 19, 571–582.

Ruiz, F., Introcaso, A., 2004. Curie point depths beneath Precordillera Cuyana and Sierras Pampeanas obtained from spectral analysis of magnetic anomalies. J. Gondwana Res. 8 (4), 1133–1142.

Ruiz, F., Introcaso, A., 2011. Study of the Claromecó Basin from gravity, magnetic and geoid undulations. Bol. Inst. Fisiograf. Geol. (UNR) 79–81, 95–106.

Ruiz, F., Luna, E., Vargas, D., Giménez, M., Martínez, P., 2011a. Importancia del ajuste y nivelación de datos aeromagnéticos a partir de magnetometría terrestre. In: 18° Congreso Geológico Argentino, 17, pp. 1198–1199.

Ruiz, F., Introcaso, A., Nacif, S., Uliarte, E., Giménez, M., Martínez, P., Leiva, F., Laplagne, A., Introcaso, A., 2011b. Cambios de gravedad de origen tectónico en la transición entre Sierras Pampeanas Occidentales y la Precordillera sanjuanina. Rev. Asoc. Geol. Argent. 68 (4), 595–605.

SEGEMAR, 1999. Grilla de datos de intensidad de campo magnético total, (17) Bloque II Precordillera Sur (San Juan – Mendoza). Servicio Geológico Minero Argentino.

SEGEMAR, 2001. Grilla de datos de intensidad de campo magnético total, (26) Área Pie de Palo (San Juan). Servicio Geológico Minero Argentino.

Siame, L., Bellier, O., Sebrier, M., 2006. Active tectonics in the Argentine Precordillera and western Sierras Pampeanas. Rev. Asoc. Geol. Argent. 61 (4), 604–619.

Siame, L.L., Bellier, O., Sébrier, M., Bourlès, D.L., Leturmy, P., Perez, M., Araujo, M., 2002. Seismic hazard reappraisal from combined structural geology, geomorphology and cosmic ray exposure dating analyses: the Eastern Precordillera thrust system (NW-Argentina). Geophys. J. Int. 150, 241–260.

Smalley Jr., R., Pujol, J., Regnier, M., Chiu, J., Chatelain, J., Isacks, B., Araujo, M., Puebla, N., 1993. Basement seismicity beneath the Andean Precordillera thin-skinned thrust belt and implications for crustal and lithospheric behavior. Tectonics 12, 63–76.

Tsokas, G., Hansen, R., 1996. A comparison between inverse filtering and multiple-source Werner deconvolution. In: 66th Annual International Meeting. SEG, pp. 1153–1156. Expanded Abstracts.

Uliarte, E., Bastías, H., Ruzycki, L., 1987. Morfología y Neotectónica en el cerro La Chilca, Pedernal. San Juan. In: 10° Congreso Geológico Argentino, 1, pp. 227–230.

Vaca, A., 1977. Contribución al conocimiento geológico del área cordón de La Flecha-cerro Valdivia, provincia de San Juan. Tesis de Licenciatura Facultad de Ciencias Exactas, Físicas y Naturales. Universidad Nacional de San Juan, p. 107 (Unpublished).

Vergés, J., Ramos, V., Meigs, A., Cristallini, E., Bettini, B., Cortés, J., 2007. Crustal wedging triggering recent deformation in the Andean thrust front between 31° S and 33° S: Sierras Pampeanas–Precordillera interaction. J. Geophys. Res. 112, B03S15. http://dx.doi.org/10.1029/2006JB 004287.

Vigny, C., Rudloff, A., Ruegg, J., Madariaga, R., Campos, J., Alvarez, M., 2009. Upper plate deformation measured by GPS in the Coquimbo gap, Chile. Phys. Earth Planet. Inter. 175 (1–2), 86–95.

Von Gosen, W., 1992. Structural evolution of the Argentine Precordillera: the Rio San Juan section. J. Struct. Geol. 14 (6), 643–667.

Vujovich, G., 2003. Metasedimentos siliciclásticos proterozoicos en la de la Sierra de Pie de Palo, San Juan: Procedencia y ambiente tectónico. Rev. Asoc. Geol. Argent 58, 608–622.

Yacimientos Petrolíferos Fiscales (YPF) S.A., 1961. Exploration Well Technical Reports. YPF-SJMA-1.

Yacimientos Petrolíferos Fiscales (YPF) S.A., 1981. Exploration Well Technical Reports. YPF-SJ-M-es-1.

Yacimientos Petrolíferos Fiscales (YPF) S.A., 1985. Exploration Well Technical Reports. YPF-SJ-SP-es-1.

Yañez, G., Ranero, C., von Huene, R., Díaz, J., 2001. Magnetic anomaly interpretation across the southern Central Andes (32°–34° S): the role of the Juan Fernandez Ridge in the late Tertiary evolution of the margin. J. Geophys. Res. Solid Earth 106, 6325–6345.

Zambrano, J., Suvires, G., 2008. Actualización en el límite entre Sierras Pampeanas occidentales y Precordillera Oriental, en la provincia de San Juan. Rev. Asoc. Geol. Argent. 63 (1), 110–116.

Zambrano, J., Victoria, J., Di Chiacchio, J., 2005. Fallas y cuencas de agua subterránea al este de la Precordillera Oriental en el sur sanjuanino. In: 20° Congreso Nacional del Agua y 3° Simposio de Recursos Hídricos del Cono Sur, pp. 1–15.

Zapata, T., 1998. Crustal structure of the Andean thrust front at 30°S latitude from shallow and deep seismic reflection profiles, Argentina. J. South Am. Earth Sci. 11 (2), 131–151.

Zapata, T., Allmendinger, R., 1996a. Evolución de la deformación del frente de corrimiento de Precordillera, provincia de San Juan. Rev. Asoc. Geol. Argent. 52 (2), 115–131.

Zapata, T.R., Allmendinger, R.W., 1996b. Thrust-front zone of the Precordillera, Argentina: a thick-skinned triangle zone. Am. Assoc. Petrol. Geol. 80 (3), 359–381.